ORIENTAL JOURNAL OF CHEMISTRY
An International Open Access, Peer Reviewed Research Journal
www.orientjchem.org
ISSN: 0970-020 X
CODEN: OJCHEG
2024, Vol. 40, No.(3):
Pg. 660-665

Clean Hydrogen Production via Methane Cracking over Ni Supported on Ceria-silica Catalysts

KANDUKURI VENKATESHWARLU[1], MANDA KALPANA[2], AYTAM HARI PADMASRI[3]*, BURRI VIJAYALAXMI[3], MAVURAPU SATYANARAYANA[1] and VASAM CHANDRA SEKHAR[1]*

[1]Department of Pharmaceutical Chemistry, Telangana University, Nizamabad–503322,Telangana, India.
[2]Catalysis and Fine Chemicals Department, CSIR–Indian Institute of Chemical Technology, Tarnaka, Hyderabad–500 007, Telangana, India.
[3]Department of Chemistry, University College of Science, Osmania University, Tarnaka, Hyderabad–500 007, Telangana, India.
*Corresponding author E-mail: csvasamsa@gmail.com, ahpadmasri@osmania.ac.in

http://dx.doi.org/10.13005/ojc/400304

(Received: April 22, 2024; Accepted: May 23, 2024)

ABSTRACT

At 550°C and atmospheric pressure, clean hydrogen was produced through CH_4 cracking on a ceria modified silica supported Ni catalyst. A high proportion of Ni surface area on 20Ni/2wt%CeO_2-SiO_2 demonstratedbetter H_2 yields. The graphitic nature of the deactivated catalyst was established by TEM, XRD analyses and the distinction between ordered and disordered carbon was established by Raman spectroscopy. The high H_2 yields produced by 20Ni/2wt%CeO_2-SiO_2 catalyst was explained due to high nickel dispersion and an improved surface area of the nickel as assessed by H_2 pulse chemisorption.

Keyword: Methane cracking, Ni supported on ceria-silica catalysts.

INTRODUCTION

The non-catalytic breakdown of methane requires very high temperatures > 1000°C to occur efficiently to obtain pure hydrogen without CO and CO_2 along with carbon. Such a carbon may be utilized as bulk amorphous activated carbon for various industrial applications[1]. Owing to the limitation of high temperature methane cracking, catalysts have been used during the previous few years to facilitate methane decomposition. Concerning the conversion of methane, generation of hydrogen and carbon,catalytic methane cracking (CMC) can be the choice as it is performed at lower temperatures between 550 to 800°C[2]. For this reason, research on carbonaceous catalysts as well as metallic catalysts has been explored[3]. Heterogeneous metal-based catalysts significantly facilitated the synthesis of hydrogen as well as the multi or single walled nano-filaments[4]. These very significant carbon nanostructures are applied in energy, including hydrogen storage and the production of electrode materials for batteries, fuel cells, super capacitors, and other devices[5]. In addition to thereduction in reaction temperature for CMC process, it was found that using a suitable

catalyst the ratio of the ordered/disordered carbon could be altered which can further enhancethe overall yield of the hydrogen[6]. A variety of factors influence the catalytic efficiency of methane decomposition catalysts. For example,metals which are functional, textural supports and or promoters, co-metals, conditions of synthesis and of catalyst preparation techniques would influence the catalyst CMC activity[7]. The most utilized active metals are Ni, Co, and Fe for the CMC process. Other d block elements were used in conjunction with promoters such as noble metals and lanthanum, magnesia, ceria, zirconia oxides etc. as supports for Ni based catalysts[8]. Furthermore, modification of the support using a suitable metal oxide could affect the catalyst stability and performance[9,10,10A]. In the present study ceria modified SiO_2 has been examined as a support for Ni catalysts for the CMC process. Reason for the selection of ceria as a modifier for SiO_2 is that its enhanced textural and redox qualities which could facilitate the dispersion of active Ni metal catalyst. Various investigations in fixed bed reactors have shown that the variables that determine conversion of CH_4 and the carbon formed includes catalyst, the sort of support, the textural properties of the catalyst, and the conditions of operation[11-13]. This study used Ni on ceria and silica to investigate the effects of catalyst textural characteristics and support type in CCM process. Characterization of the catalysts is performed by various techniques such as Temperature programmed reduction by H_2TPR, SA by N_2 physisorption, spectroscopy study of carbon by Raman, X-ray diffraction study by XRD, carbon, hydrogen, nitrogen, and sulfur content study by CHNS, and chemisorption by hydrogen pulse. The physicochemical characterization data deduced from the above techniques was utilized to correlate with H_2 production rates.

EXPERIMENTAL

Different loadings (2, 4, 6, 8 and 10wt%) of CeO_2 is impregnated over fumed silica as a support and calcined in flowing air at 550°C. $Ni(NO_3)_2.6H_2O$ is used as a precursor for a Ni loading of 20wt%which was impregnated on the varied loadings of CeO_2-SiO_2 support. At 550°C, the calcination of the catalysts is performed and reduced at the same temperature in H_2 flowbefore being examined for the CMC reaction. In a standard procedure a known quantity of nitrate of Ni is dissolved in raw water to which a desired amount of CeO_2-SiO_2 support was added and stirred at 80°C. Evaporation of water from the samples was at 120°C in an oven and subsequent calcination at required temperature (550°C).

Characterization

For conciseness and to prevent self-plagiarism, the experimental details pertaining to the BET surface area, XRD, SEM, TEM, H_2 TPR, H_2-pulse chemisorption, CHNS analysis, and Raman spectroscopy techniques are described in supplementary material.

CH_4 cracking studies

Calcined 20wt%Ni/CeO_2-SiO_2 catalyst (~ 0.1 g) is loaded in the centre of a fixed bed quartz reactor. A mixer with 5% H_2 balance Ar was used for the reduction of the catalyst for 3 h at 550°C before the reaction began. Subsequently, the 5% H_2/Ar gas was replaced with 30 mL/min of CH_4 flowing over the catalyst at 550°C[14]. N_2 is employed as the gas carrier and the reactor exit product stream was examined using a Shimadzu gas chromatograph (thermal conductivity detector; column-carbosphere/carboxen). Aautosampler with six ports is used to analyse the methane conversion with a time interval of 20 minute. Until the hydrogen peak is negligible and the methane content found constant, the reaction is performed. Carbon oxides (CO and/or CO_2) were not found during the course of reaction emphasizing the methane cracking led to exclusive formation of H_2. Cross-checking was done on the hydrogen yields determined by measuring CH_4 conversion and H_2 production and CHNS analysis for the carbon that accumulated from the recovered catalyst. The mass balance is confirmed by the lack of compounds such as CO and/or CO_2 during the process and these results are in accordance with the recent reports on the CMC reaction[15].

RESULTS AND DISCUSSION

N_2 physisorption analysis

N_2 Physisorption results show decrease in the surface area as the percentage loading of CeO_2 increases, possibly because of the silica support pores becoming blocked. The results are tabulated below.

Table 1: Physicochemical characteristics of 20wt%Ni supported on CeO_2-SiO_2

CeO_2(wt%) in SiO^2	BET-SA (m_2/g)[a]	Crystallite Size(NiO)[b]	H_2 uptake (mmol/g)[c]	H_2 uptake (cm^3/g)[d]	Ni metal surface area (m^2/g)[e]	H_2 Yields (molH^2/mol Ni)
2	142	18.4	3.33	0.12	2.75	2136
4	139	18.1	3.41	0.05	2.2	1163
6	130	18.3	3.51	0.09	2.12	1575
8	128	17.9	3.89	0.06	2.01	767
10	117	18	5.23	0.05	1.99	573

[a]calculated from BET surface area; [b]XRD analysis; [c]H_2TPR; [d,e]H_2 pulse chemisorption

XRD analysis of the fresh and deactivated catalysts

The 20wt%Ni/CeO_2-SiO_2 patterns of XRD that were calcined at 550°C are shown in Fig. 1A. The presence of NiO phase is explained from the reflections appeared at 2θ=37.28, 43.3 and 62.9°, with 1.48, 2.09 and 2.41A°'d' values [ICDD#01-1239]. The diffraction peak at 14.5°, is corresponding to CeO_2 phase. The deactivated catalysts XRD showed the reflections of graphitic carbon and Ni only (Figure 1B).

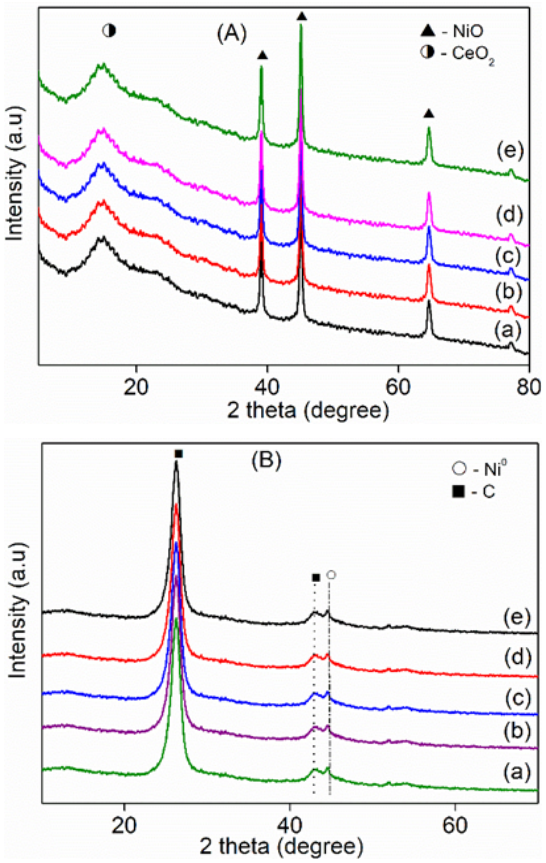

Fig. 1. XRD patterns of (A) fresh and (B) deactivated samples of 20wt%Ni over (a) 2 (b) 4 (c) 6 (d) 8 (e) 10wt%CeO_2-SiO_2 catalysts

H_2-TPR

The metal oxides reduction behaviour is investigated using H_2-TPR (Fig. 2) analysis, and Table 1 provides a list of pertinent hydrogen uptakes over 20wt%Ni/CeO_2-SiO_2 catalysts. In every sample, a broad peak was discernible due to the reduction of NiO and certain ratio of CeO_2 species. The bulk feature of the H_2-TPR technique was demonstrated by the increased H_2 consumptions with increasing CeO_2 loadings due to the presence of CeO_2 species that were appeared in XRD analysis (Fig. 1A). The signals Tmax is somewhat shifted towards a high temperature as CeO_2 loading is increased. This is probably due to an interaction between nickel and ceria particles. XRD analysis specifies that the size of nickel crystal is similar over these catalysts. However, having a constant loading of Ni (20wt%) a raise in H_2 uptakes are found upon increasing the CeO_2 loadings, indicating that ceria species were undergone during the TPR (Table 1). Furthermore, the shoulder peak tail extended towards higher temperatures from CeO_2 loadings 2 to 10wt% is noticed. The interaction of NiO species with the CeO_2 could causethis peak shift.

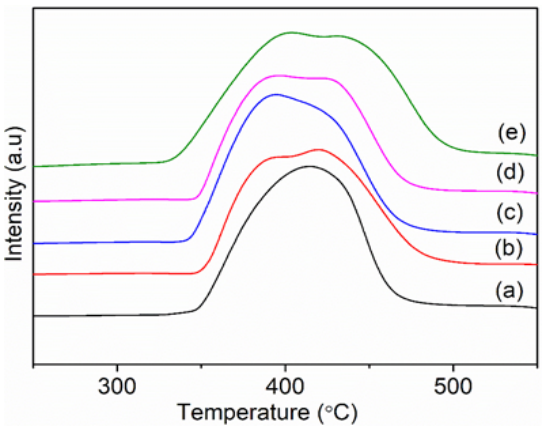

Fig. 2. H_2 TPR patterns of 20wt%Ni supported on (a) 2 (b) 4 (c) 6 (d) 8 and (e) 10wt%CeO_2-SiO_2 catalysts

H_2 chemisorption

Using chemisorption by H_2, the metallic Ni area was determined. Itdecreased from 2.75-1.99 m^2 g^{-1}, upon increasing the CeO_2 loadings on SiO_2 as seen by the H_2 adsorption data (Table 1). The 20wt%Ni/2wt% CeO_2-SiO_2 catalyst showed a high proportion of dispersed nickel species on the surface. Low temperature reduction enhances the Ni dispersion over the catalyst surface.

CH_4 cracking activity

Figure 3 displays the CCM activity with time operated at 550°C on the 20wt%Ni supported on various loadings of CeO_2 on SiO_2 catalysts.All the catalysts get deactivated with time. The catalyst with lower CeO_2 loading displayed better sustainability compared to other loadings. Table 1 provides the H_2 yields that were obtained during the CMC reaction. High initial conversion, followed by a deactivation within 15 h, is evident from the activity data. At a higher loading of CeO_2 (10wt%), the catalyst was deactivated quickly within 8 h on stream producing lower hydrogen yields. Compared to the other catalysts, 20Ni/2wt%CeO_2-SiO_2 exhibited higher activity. It has been found that there is a good correlation between the yields of H_2 and SA of nickel over these catalysts (Table 1). All the catalysts recovered after the reaction was analysed by TEM and Raman spectroscopy to understand the nature and type of carbon formed.

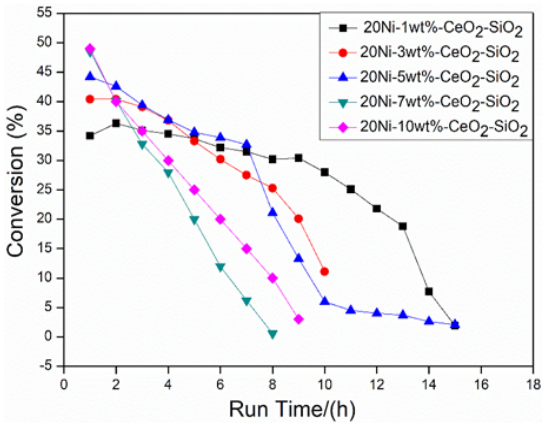

Fig. 3. Time on stream analysis of CMC activity over 20wt%Ni supported on CeO_2-SiO_2

Characterization of deactivated catalysts by TEM and Raman spectroscopy

The transmission electron microscopic images of the 20Ni/2wt%CeO2-SiO_2 catalyst is reported in Fig 4. Fig. 4A clearly shows carbon nano fibre with tip growth mechanism. With a diameter of around 40 nm CNFswere seen in TEM images (Fig. 4A and 4B). The growth of the CNT is dependent on the particle size of Ni[16]. Catalyst interior, with carbon strand behaviour and diffusion in a 'V' shape, was visible in the TEM image (Fig. 4C and 4D). The similar size of carbon nanofiber and the Ni particle is observed.

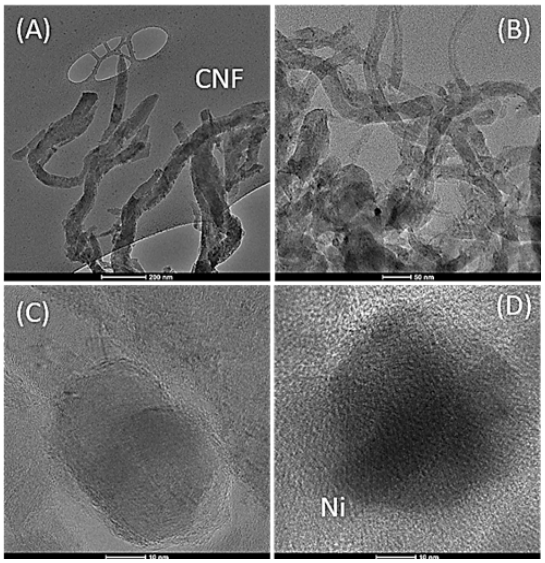

Fig. 4. TEM images of the deactivated 20Ni/2wt%-CeO_2-SiO_2 catalyst recovered after 15 hour

Raman spectroscopic results

Figure 5 reports the Raman spectra of the 20Ni/CeO_2-SiO_2 catalysts recovered after the reaction which showsboth the “D” and “G” bands of carbons. Two distinct bandswere shown, one at approximately 1320 cm^{-1} which is explained by amorphous and carbon nanoparticles or disordered carbon due to structural defects in graphite. The G-band roughly 1580 cm^{-1} is by in-plane stretching of carbon vibrations by ordered structure of C[17,18]. The D band full width at half maximum (FWHM) to the ordered band I_D/I_G is correlated negativelywith the graphene[19]. This shows higher ordered nature similar to graphene at lower I_D/I_G values. When FWHM increased, the ratio of disordered to ordered is decreased. For carbon nanofibers, Alvarez *et al.,* discovered a comparable relationship between full width half maxima and the ratio[20]. The build-up of C versus the width of G-band suggests the formation of ordered carbon over 20Ni/2wt%-CeO_2-SiO_2. The ordered carbon deposition explained due to the high CMC activity of the 20Ni/2wt%-CeO_2-SiO_2 catalystin comparison to other catalysts.

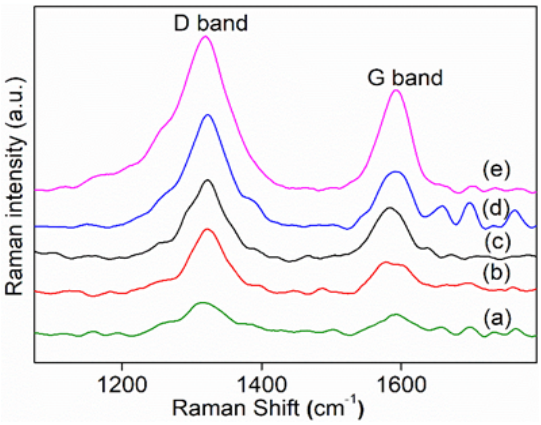

Fig. 5. Raman spectra of the 20wt%Ni supported on (a) 2 (b) 4 (c) 6 (d) 8 and (e) 10wt%CeO_2-SiO_2 catalysts

The carbon form determined with Raman spectroscopic analysis emphasizes reasons why a particular catalyst system show rate of hydrogen production. According to Scott *et al.,* combining silica with ceria for methane dry reforming improves the performance of Ni-based catalysts[21]. Their work elaborates on the features of the catalyst that are determined by the composition and structure of the support. Yoshida and colleagues carried out non-oxidative coupling of methane over supported ceria photocatalysts[22]. A range of rare earth oxides supported by silica was investigated for photocatalytic methane conversion. Of these, the cerium oxide supported by silica with lower loading demonstrated the highest photo activity to generate hydrogen and ethane[22]. According to Wang *et al.,* effects of size and sturdy metal support interaction contributes to good performance for methane dry reforming[23]. Takriff *et al.,* investigated the reforming of CH_4 using ceria as a support material and Pt as a promoter[24]. In this study we found an improved rate of hydrogen on a silica that is modified with 2wt%CeO_2 as a support for Ni loading of about 2136 mole of H_2 per mole of Ni. Excess addition of CeO_2 to SiO_2 caused the decrease in surface areas as well as the Ni metal surface areas can be a possible reason for the lower hydrogen rates while maintaining a constant weight percentage of Ni (Table 1). The decrease in surface areas could potentially be due to Ni-CeO_2 interaction.The bulk property of the catalyst is explained by the rise in H_2 uptake values with increase in CeO_2 loading as observed from the H_2-TPR data (Table 1). The interaction between Ni and CeO_2 seems to be weak at a loading of 2wt% as the H_2 TPR displayed a broad single peak. However, the peak split is noted from 4-10wt% of CeO_2 loaded SiO_2 supported Ni catalysts (Fig. 2). The fine metal dispersion in 2wt%CeO_2–SiO_2 can be explained by the high metallic surface area compared to other CeO_2 loadings. The 2wt%CeO_2 produced high H_2 yields of 2136 mol H_2/mol Ni at 550°C and atmospheric pressure, wherein excess addition of CeO_2 with 4wt% and higher leads to low H_2 yields of about 573 moles of H_2 per mole of Ni over 20wt%Ni/10wt%CeO_2-SiO_2 catalyst. The 20wt%Ni/10wt%CeO_2-SiO_2 deactivated catalysts displayed more carbon which is graphitic with a lower ID/IG ratio.

CONCLUSION

In summary, the Ni supported on CeO_2 modified SiO_2 catalyst was found to be an active catalyst for CH_4 cracking at moderate temperatures to produce pure hydrogen and carbon nanofibers. Yields of H_2 agree with SA of nickel of the corresponding CeO_2 loaded SiO_2 supported Ni catalysts. The 20Ni/2wt%CeO_2-SiO_2 catalyst exhibited higher methane cracking performance in comparison to other catalysts. The spent catalyst is characterized by XRD and TEM analysis which showed filamentous carbon. Thecrystalline and amorphous carbon domains were manifestedby Raman spectra. The higher hydrogen yields obtained over 20Ni/2wt%CeO_2-SiO_2 was explained due to the high nickel SA and formation of well-ordered carbon.

ACKNOWLEDGMENT

The authors acknowledge the Department of Chemistry, Osmania University, Hyderabad and Telangana University, Nizamabad for providing research facilities.

Conflict of Interest

There is no conflict of interest

REFERENCES

1. Soo Kim, I. K.; Eun, S. C.; Sang, W. K.; Seok Lee, C.; Junyoung, K.; Eun Byun, K.; Unyong., *J. Adv. Mater.,* **2022**, *35*, 43.
2. Yousefi, M.; Donne, S., *Int. J. Hydrogen Energy*., **2022**, *47*, 699-727.
3. Torres, D.; Pinilla, J.L.; Lazaro, M. J.; Moliner, R.; Suelves, I., *Int. J. Hydrogen Energy*., **2014**, *39*, 3698–3709.

4. Suelves, I.; Pinilla, J. L.; Lázaro, M. J.; Moliner, R.; Palacios, J. M., *J. Power Sour.,* **2009**, *192*, 35–42.
5. Abbas,H. F.; Daud, W. M. A., *Int. J. Hydrogen Energy*., **2010**, *35*, 1160–1190.
6. Kalpana, M.; Manasa, K.; Padmasri, H. A.; Pratyay, B.; Akella, V. S.; Venugopal, A., *EP & SE*., **2023**, *14*, 41-49.
7. Li,Y.; Li,D.; Wang, G., *Catal. Today*., **2011**, *162*, 1–48.
8. Ashik, U. P. M.; Daud,W. M. A. W.; Hayashi, *J. Renewable Sustainable Energy Rev*., **2017**, *76*, 743–767.
9. Pinilla, J. L.; Moliner, R.; Suelves, I.; Lazaro, M.J.; Echegoyen,Y.; Palacios, J. M., *Int. J. Hydrogen Energy*., **2007**, *32*, 4821-4829.
10. Takenaka, S.; Ogihara, H.; Yamanaka, I.; Otsuka, K., *Appl. Catal. A.*, **2001**, *217*, 101-10.
10A. Borges R.P.; MouraL.G.; Kanitkar S.; Spivey J.J.; Noronha F.B.; Hori C.E., *Cat. Today*., **2021**, *381*, 3-12.
11. Spiess, F. J.; Suib, S. L.; Irie, K.; Hayashi, Y.; Matsumoto, H., *Catal. Today*., **2004**, *89*, 35-45.
12. Li, Y.; Zhang, B.; Xie, X.; Liu, J.; Xu,Y.; Shen, W., *J. Catal.,* **2006**, *238*, 412-24.
13. Ashok, J.; Naveen Kumar, S.; Venugopal, A.; Durga Kumari,V.; Subrahmanyam, M., *J. Power Sources.*, **2007**, *164*, 809-14.
14. Wei,Y.; Kent, H. S., *Environ. Prog. & Sustain*., **2014**, *33*, 213-219.
15. Manasa, K.; Naresh, G.; Kalpana, M.; Sasikumar, B.; Vijay Kumar, V.; Chary, K.V.R.; Michalkiewicz,B.; Venugopal. A., *J. Energy Inst.*, **2021**, *99*, 73-81.
16. Naresh, G.; Vijay Kumar, V.; Anjaneyulu, C.; Tardio, J.; Bhargava, S. K.; Patel, J.; Venugopal, A., *Int. J. Hydrogen Energy*., **2016**, *41*, 19855-62.
17. Dussault, L.; Dupin, J. C.; Guimon, C.; Monthioux, M.; Latorre, N.; Ubieto, T.; Romeo, E.; Royo,C.; Monzon, A., *J. Catal*., **2007**, *251*, 223.
18. Li, Y.; Zhang, B. C.; Xie, X. W.; Liu, J.L.; Xu,Y.D.; Shen, W.J., *J.Catal*., **2006**, *238*, 412.
19. Darmstadt, H.; Summchen, L.; Ting, J.M.; Roland, U.; Kaliaguine, S.; Roy, C., *Carbon*., **1997**, *35*, 1581.
20. Alvarez, W.E.; Pompeo, F.; Herrera, J. E.; Balzano,L.; Resasco, D.E., *Chem Mater*., **2002**, *14*, 1853.
21. Lovell, E. C.; Horlyck, J.; Scott, J.; Amal, R., *Applied Catal. A: General*., **2017**, *547*, 47-57.
22. Yuliati, L.; Hamajima,T.; Hattori, T.; Yoshida, H., *J. Phys. Chem. C.,* **2008**, *112*(18), 7223–7232.
23. Han, K.; Xu, S.; Wang, Y.; Wang, S.; Zhao, L. *J. Power Sources*., **2021**, *506*, 230-232.
24. Pudukudy, M.; Yaakob, Z.; Jia, Q.; Takriff, M. S., *New J. Chem*., **2018**, *42*, 14843-14856.